Short communication

Electrooxidation of ethanol on novel multi-walled carbon nanotube supported platinum–antimony tin oxide nanoparticle catalysts

Dao-Jun Guo[*]

School of Chemistry and Chemical Engineering, The Key Laboratory of Life-Organic Analysis, Qufu Normal University, Qufu, Shandong 273165, PR China

ABSTRACT

We synthesize the new Pt based catalyst for direct ethanol fuel cells using novel multi-walled carbon nanotubes supported platinum–antimony tin oxide (Pt–ATO/MWCNT) nanoparticle as new catalyst support for the first time. The structure of Pt–ATO/MWCNT catalyst is characterized by transmission electron micrograph (TEM) and X-ray diffraction (XRD). The electrocatalytic properties of Pt–ATO/MWCNT catalyst for ethanol electrooxidation reactions are investigated by cyclic voltammetry (CV) and chronoamperometric experiments in acidic medium. The electrocatalytic activity for ethanol electrooxidation reaction shows that high carbon monoxide tolerance and good stability of Pt–ATO/MWCNT catalyst compared with Pt–SnO_2/MWCNT and commercial Pt/C are observed. These results imply that Pt–ATO/MWCNT catalyst has promising potential applications in direct alcohol fuel cells.

© 2010 Elsevier B.V. All rights reserved.

1. Introduction

Direct alcohol fuel cells (DAFCs) is a promising technology as an alternative to conventional energy-generating devices due to its higher energy-conversion efficiency, low-to-zero pollutant emissions, ready availability of alcohol fuel, ease in distribution, and high energy density [1,2]. The commercialization of DAFCs, however, is still significantly restricted by its high cost, mainly caused by the low utilization of novel metal in the catalytic electrode. The electrocatalytic activity towards noble metals for alcohol oxidation is greatly dependent on many factors such as the size and dispersion of noble metals, properties of supporting materials and synthetic methods [3,4]. Among them, the properties of supporting materials and their surface characteristics are essential for the catalysts materials to produce high catalytic activity [5,6].

Nanostructured carbon materials, especially one-dimensional (1D) carbon nanotubes (CNTs), appear to be one of the most promising supporting materials, such as for new chemical nanoarchitectures in electrocatalysis [7,8] and nanoelectronic circuitry [9], due to their unique structure and excellent mechanical, electronic and surface properties [10]. Much work has focused on the dispersion of metal nanoparticles on the surface of CNTs as catalysts for fuel cells. Much work has focused on synthesis of highly dispersed metal nanoparticles on the surface of CNTs as catalysts for fuel cells [7,9,11–13].

Recently, another strategy by using some other metal oxides such as CeO_2, ZrO_2, TiO_2 and so on modified (or coated) carbon black (CB) or carbon nanotube (CNT) as the support of Pt catalysts have also been developed, in which the metal oxides can also enhance the CO tolerance of the catalysts according to the bifunctional mechanism [14–18]. The results reported in the literature confirm that these fillers are indeed effective in improving the catalytic activity of Pt catalyst. But Pt deposits on the surface of metal oxides, which may be useless due to the bad electron conductivity of metal oxide. To solve this problem and increase the utilization of Pt catalysts, alternative materials with high electron conductivity are strongly aspired for. In the same way, antimony doped SnO_2 (ATO) has been proposed as a support material for fuel cell electrocatalysts because of its chemical properties: it adsorbs OH species at low potentials and/or induces the electronic effect with Pt catalysts. These properties promote the electrooxidation on Pt of CO and low molecular-weight alcohols, such as methanol [19] and ethanol [20]. The electroactivity of Sb–SnO_2 supported Pt was investigated by electrochemical method and compared to the activity of platinized platinum. Pt/ATO electrodes not only presented higher roughness factors than platinized Pt electrodes, but also had larger intrinsic electrocatalytical activity for the electrooxidation of alcohol [19].

It is well known that the supported metal nanoparticles show a higher electrocatalytic activity and utilization efficiency than unsupported metal particles because of their large surface area on the supports [21]. Hence, in this study, Pt nanoparticle contacting with adjacent ATO supported on the multi-walled carbon nanotubes was prepared by a consecutive polyol process with aiming to the high activity for the ethanol oxidation reaction.

* Tel.: +86 537 4453161; fax: +86 537 4456305.
E-mail address: guodaojun03@163.com.

2. Experimental

2.1. Preparation of Pt–ATO/MWCNT catalysts

The ATO/MWCNT composites were synthesized as follows. First, 100 mg of $SnCl_4 \cdot 5H_2O$, 3.4 mg of $SbCl_3$ (5 at% to Sn), 0.05 mL HCl (37%), and deionized (DI) water with appropriate amounts of MWC-NTs were mixed to homogeneity. Then an aqueous solution of ammonia was added until pH 10. The solution was moved to a three-necked flask and refluxed at 100 °C for 2 h in inert atmosphere. After refluxing, the solution was cooled, centrifuged, and evaporated. The dark-yellow solid thus obtained was heated in a tube furnace at 400 °C for 1 h in ambient air. The ATO content was 50% by weight in the catalyst supports. For comparison, the SnO_2/MWCNT composites were also obtained with the same process without Sb added.

Preparation of Pt–ATO/MWCNT nanoparticles was based on the polyol method [22]. Appropriate $H_2PtCl_6 \cdot 6H_2O$ ethylene glycol solution (0.02 M) was mixed with NaOH ethylene glycol solution (0.1 M). Ethylene glycol was used as a stabilizer and reducing agent. ATO/MWCNT supports were then added to the mixed solution and sonicated for 15 min. Then the solution was stirred at 130–140 °C for 4 h. The reaction mixture was cooled to room temperature and dripped with KNO_3 (0.1 M) and HCl (0.5 M) successively for 4 h. After stirring overnight, the product was collected by centrifugation, washed several times with water and ethanol, and dried in a vacuum oven at 70 °C overnight and then the Pt–ATO/MWCNT catalysts with 20 wt% Pt on ATO/MWCNT support were obtained. For comparison, Pt supported on SnO_2/MWCNT composites (Pt–SnO_2/MWCNT) with the same contents of Pt nanoparticles was also obtained.

2.2. Measurement

Electrochemical reactivity of the catalysts was measured by CV using a three-electrode cell at the PARSTAT 2273 potentiostat controlled by PowerSuite® software (Princeton Applied Research). Thin film working electrodes were prepared by dispersing 20 mg of Pt–ATO/MWCNT in deionized water and isopropyl alcohol, ultra-sonicating for 30 min, and pipeting out 10 mL of the resulting suspension on a gold substrate (1 cm² surface) using a micropipette followed by drying in air and adding 5 mL of 5% Nafion solution as a binder to affix the electrocatalysts firmly to the gold plate, the solvent was allowed to evaporate slowly. Pt gauze and a saturated calomel electrode (SCE) were used as counter electrode and reference electrode. All potentials in this report are quoted versus SCE. CV test was conducted at 50 mV s⁻¹ in a solution of 1 M H_2SO_4 with 1 M CH_3CH_2OH, potential ranging from −0.2 to 1.4 V. The electrochemical measurements were conducted under 25 °C.

The morphology of Pt–ATO/MWCNT composites were investigated using high-resolution transmission electron microscopy (JEOL model JEM-2100) operated at 200 kV. The XRD patterns of the as-prepared products were investigated via a Bruker powder diffraction system (model D8 Advanced), using Cu K_α as the radiation source at the operating voltage of 40 kV and a scan rate of 6° min⁻¹.

3. Results and discussion

3.1. TEM analysis of the Pt–ATO/MWCNT composites

Fig. 1 shows the typical HRTEM images of the Pt–ATO/MWCNT composites. It can be seen that the Pt and ATO nanoparticles are uniformly distributed on the surface of the MWCNTs. The diameter of the Pt or ATO nanoparticles is about only 3–8 nm. Thus, the HRTEM
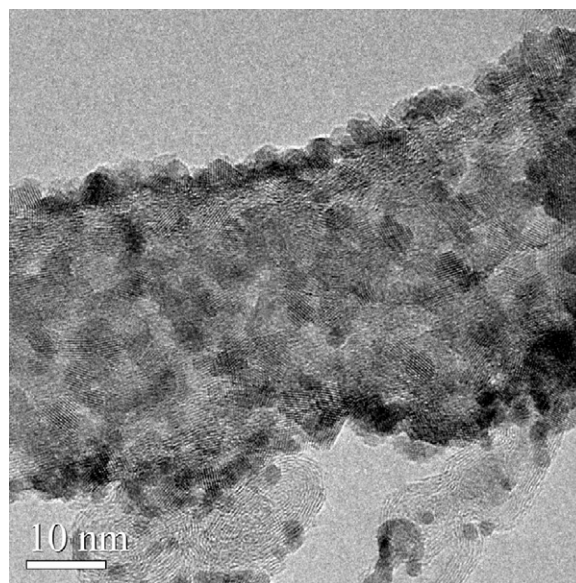

Fig. 1. HRTEM images of Pt–ATO/MWCNT composites.

micrograph reveals further that both Pt and ATO nanoparticles attached on the sidewalls of the MWCNTs, Pt and ATO nanoparticles can be identified from the crystal lattice pattern, and the presence of Pt and ATO nanoparticles can be further confirmed in the XRD results. In general, there are at least three cases for Pt nanoparticles location on MWCNT surface. The first case is that some Pt catalysts are deposited on MWCNT surface with no contact with ATO. The second case is that some Pt nanoparticles have contacts closely with ATO. The last case is that some Pt nanoparticles are deposited on the surface ATO. Because of excellent conductivity of ATO compared with the SnO_2 nanoparticle, these Pt catalysis supported on ATO can also been used for ethanol electrooxidation in fuel cell.

3.2. XRD analysis of the Pt–ATO/MWCNT composites

Fig. 2 shows the XRD patterns of Pt–ATO/MWCNT and ATO/MWCNT. For the patterns of Pt–ATO/MWCNT, both diffraction peaks of Pt and ATO can be observed indicating their coexistence in the sample. The characteristic peaks of face centered cubic
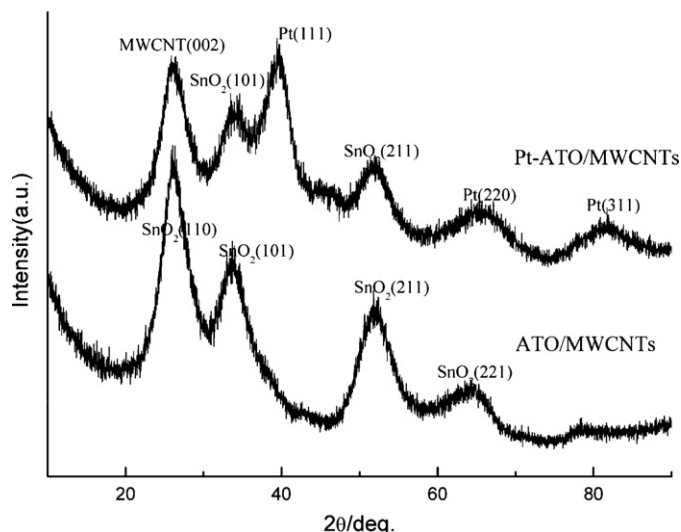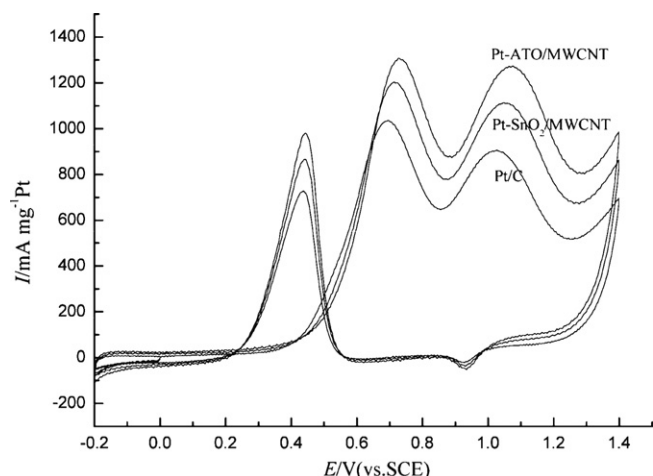

**Fig. 2.** XRD analysis of Pt–ATO/MWCNT and ATO/MWCNT composites.

Fig. 3. Cyclic voltammograms of various electrodes at $50\,mV\,s^{-1}$ in $1.0\,M$ $H_2SO_4 + 1.0\,M\ CH_3CH_2OH$ aqueous solution.

crystalline platinum at about $39°$, $46°$, $68°$ and $81°$, are corresponding to Pt (1 1 1), (2 0 0), (2 2 0) and (3 1 1) plane, respectively. And there is no shift in any of the diffraction peaks of platinum in Pt–ATO/MWCNT catalyst indicating that the addition of ATO has no effect on the crystalline lattice of platinum. The breadth of the XRD peaks also indicated that small Pt and ATO crystallites were obtained. The average crystal size of Pt and ATO nanoparticles estimated using Scherrer equation was about 3.6 and 8.2 nm, respectively, which is confirmed by HRTEM micrographs.

3.3. Electrochemical properties of Pt–ATO/MWCNT composites

The electrocatalytic activities of the catalysts toward ethanol oxidation measured by cyclic voltammetry at a potential scan rate of $50\,mV\,s^{-1}$ are shown in Fig. 3. The ethanol oxidation activity could be reflected by the magnitude of the anodic peak current in the forward scan. The peak current densities (mass catalytic activities) obtained at the potential of about 0.70 V in the forward scan for Pt–ATO/MWCNT, Pt–SnO$_2$/MWCNT, and Pt/C are 1300, 1198, and $1036\,mA\,mg^{-1}$ Pt, respectively, which have been normalized to the total metal Pt loadings. In comparison with Pt/C, the 25% increase in the catalytic activity for catalyst Pt–ATO/MWCNT strongly suggests the significant role of the ATO nanoparticles. Moreover, compared with Pt–SnO$_2$/MWCNT, the 8.5% increase for Pt–ATO/MWCNT may be related to the ATO nanoparticles with higher conductivity on the MWCNT wall. Thus, ATO has the higher conductivity compared with the SnO$_2$, as support for a Pt catalyst may facilitate increasing the utilization of the catalyst for ethanol oxidation.

The electrochemical stability of these electrodes for ethanol electrooxidation was investigated by chronoamperometric experiments at room temperature as shown in Fig. 4. The potential was first held at -0.1 V from the open-circuit potential for 100 s and then stepped up to 0.55 V for 3600 s. In general, ethanol was continuously oxidized on the catalyst surface, and tenacious reaction intermediates such as CO$_{ads}$ would begin to accumulate if the kinetics of their removal could not keep pace with that of ethanol oxidation. A more gradual decay of current density with time is therefore an indicative of improved CO tolerance. Thus, the decay rate of Pt–ATO/MWCNT and Pt–SnO$_2$/MWCNT for the oxidation current density was about the same whereas the decay rate for Pt/C was less moderate. This is an indication that the CO tolerance of Pt–ATO/MWCNT is comparable to that of Pt–SnO$_2$/MWCNT but better than that of Pt/C, consistent with the result shown in Fig. 3. The steady-state current densities at the end of 3600 s for Pt–ATO/MWCNT, Pt–SnO$_2$/MWCNT, and Pt/C are 63, 32, and
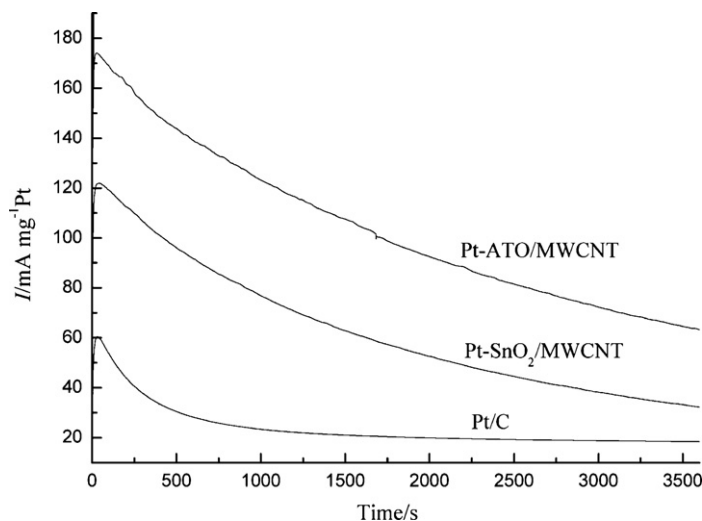
Fig. 4. Chronoamperograms of various electrodes at 0.55 V in $1.0\,M\ H_2SO_4 + 1.0\,M$ CH_3CH_2OH aqueous solution.

$17\,mA\,mg^{-1}$ Pt, respectively. The Pt–ATO/MWCNT catalyst using ATO/MWCNT nanocomposite as the support exhibits the highest activity, consistent with the CV curves shown in Fig. 3. This may imply that the ATO/MWCNT support with higher conductivity enhances the utilization of Pt electrocatalysts for the ethanol electrooxidation reaction.

4. Conclusions

In summary, a novel nanostructured electrocatalyst (Pt–ATO/MWCNT) with Pt nanoparticles supported on the ATO/MWCNT nanocomposite was fabricated. Pt nanoparticles were highly dispersed on the surface of ATO/MWCNT composites. The electrocatalytic activity and utilizaton of Pt–ATO/MWCNT for ethanol electrooxidation was better than that of Pt–SnO$_2$/MWCNT and commercial Pt/C catalysts. Its CO tolerance performance is comparable to that of Pt–SnO$_2$/MWCNT but largely improved compared with commercial Pt/C. The enhanced properties could be interpreted by the bifunctional mechanism, the synergetic interaction of between Pt and ATO nanoparticles and the higher conductivity of ATO/MWCNT compared with SnO$_2$/MWCNT composties.

References

[1] T.C. Deivaraj, W.X. Chen, J.Y. Lee, J. Mater. Chem. 13 (2003) 2555–2560.
[2] W.M. Wang, D. Zheng, C. Du, Z.Q. Zou, X.G. Zhang, B.J. Xia, H. Yang, F.D.L. Akins, J. Power Sources 167 (2007) 243–249.
[3] Z.L. Liu, X.Y. Ling, X.D. Su, J.Y. Lee, J. Phys. Chem. B 108 (2004) 8234–8240.
[4] S.H. Joo, S.J. Choi, I. Oh, J. Kwak, Z. Liu, O. Terasaki, et al., Nature 412 (2001) 169–172.
[5] E.S. Steigerwalt, G.A. Deluga, D.E. Cliffel, C.M. Lukehart, J. Phys. Chem. B 105 (2001) 8097–8101.
[6] D.J. Guo, H.L. Li, J. Electroanal. Chem. 573 (2004) 197–202.
[7] G. Wu, Y.S. Chen, B.Q. Xu, Electrochem. Commun. 7 (2005) 1237–1243.
[8] Z.B. He, J.H. Chen, D.Y. Liu, H.H. Zhou, Y.F. Kuang, Diamond Relat. Mater. 13 (2004) 1764–1770.
[9] K. Jurkschat, S.J. Wilkins, C.J. Salter, H.C. Leventis, G.G. Wildgoose, L. Jiang, T.G.J. Jones, A. Crossley, R.G. Compton, Small 2 (2006) 95–98.
[10] K.H. An, W.S. Kim, Y.S. Park, J.M. Moon, D.J. Bae, S.C. Lim, Y.S. Lee, Y.H. Lee, Adv. Funct. Mater. 11 (2001) 387–392.
[11] T. Maiyalagan, B. Viswanathan, U.V. Varadaraju, Electrochem. Commun. 7 (2005) 905–912.

[12] S.D. Yang, X.G. Zhang, H.Y. Mi, X.G. Ye, J. Power Sources 175 (2008) 26–32.
[13] Z.W. Zhao, Z.P. Guo, J. Ding, D. Wexler, Z.F. Ma, D.Y. Zhang, H.K. Liu, Electrochem. Commun. 8 (2006) 245–250.
[14] H.Q. Song, X.P. Qiu, F.H. Li, Electrochim. Acta 53 (2008) 3708–3713.
[15] H.J. Kim, D.Y. Kim, H. Han, Y.G. Shui, J. Power Sources 159 (2006) 484–490.
[16] Y.X. Bai, J.J. Wu, J.Y. Xi, J.S. Wang, W.T. Zhu, L.Q. Chen, X.P. Qiu, Electrochem. Commun. 7 (2005) 1087–1090.
[17] M. Takahashi, T. Mori, F. Ye, A. Vinu, J. Am. Ceram. Soc. 90 (2007) 1291–1294.
[18] J.S. Wang, J.Y. Xi, Y.X. Bai, Y. Shen, J. Sun, L.Q. Chen, W.T. Zhu, X.P. Qiu, J. Power Sources 164 (2007) 555–560.
[19] A.L. Santos, D. Profeti, P. Olivi, Electrochim. Acta 50 (2005) 2615–2621.
[20] K.-S. Lee, I.-S. Park, Y.-H. Cho, D.-S. Jung, N. Jung, H.-Y. Park, Y.-E. Sung, J. Catal. 258 (2008) 143–152.
[21] N. Chakroune, G. Viau, S. Ammar, L. Poul, D. Veautier, M.M. Chehimi, C. Mangeney, F. Villain, F. Fievet, Langmuir 21 (2005) 6788–6796.
[22] X. Guo, D.J. Guo, X.P. Qiu, L.Q. Chen, W.T. Zhu, Electrochem. Commun. 10 (2008) 1148–1151.